buildings

MDPI

Article

Effect of Orientation and Skylight Area Ratio on Building Energy Efficiency in the Qinghai–Tibet Plateau

Yingmei Wang [1,2], Haosen Qin [1,2], Yan Wang [3], Ji Chen [4,*], Xin Hou [4], Pengfei Rui [4], Shouhong Zhang [5] and Hanyu Song [6]

1 School of Energy and Power Engineering, Lanzhou University of Technology, Lanzhou 730050, China
2 Key Laboratory of Complementary Energy System of Biomass and Solar Energy, Lanzhou 730050, China
3 School of Materials Science and Engineering, Wuhan University of Technology, Wuhan 430070, China
4 Beiluhe Observation and Research Station of Frozen Soil Engineering and Environment, State Key Laboratory of Frozen Soil Engineering, Northwest Institute of Eco–Environmental and Resources, Chinese Academy of Sciences, Lanzhou 730000, China
5 China Railway Qinghai–Tibet Group Co., Ltd., Xining 810007, China
6 Shangqiu Branch of China Tower Co., Ltd., Shangqiu 476000, China
* Correspondence: chenji@lzb.ac.cn

Abstract: The Qinghai–Tibet plateau, with an average altitude of over 4000 m, has low annual average temperatures and a high demand for building heating. This region's abundant solar energy resources hold substantial practical significance for improving the indoor heat environment and reducing building energy consumption. This paper investigates the impact of orientation and skylight area ratio on building heat load and indoor temperature, using both actual measurement and simulation methods, with a case study of the comprehensive building at Beiluhe Observation and Research Station of Frozen Soil Engineering and Environment (Beiluhe Station), located in the Qinghai–Tibet Plateau region. Initially, a model was established using the EnergyPlus 9.4 software, with orientation variables set from east to west in 15° increments, to simulate the variations in building heat load resulting from orientation changes; simulations were then conducted for three different skylight area ratios under the optimal orientation to evaluate their influence on heat load and indoor temperature. The results show that for the architectural style examined in this paper, the optimal building orientation within the region is 30° south by east, with the optimal orientation range spanning from 45° south by east to due south. Heating load is negatively correlated with the skylight area ratio, and beyond a certain threshold, the rate of decrease in heat load diminishes or even stabilizes. The conclusions of this paper offer guidance for the orientation and skylight design of new buildings on the Qinghai–Tibet Plateau.

Keywords: building orientation; skylight area ratio; Qinghai–Tibet plateau; Beiluhe station

Citation: Wang, Y.; Qin, H.; Wang, Y.; Chen, J.; Hou, X.; Rui, P.; Zhang, S.; Song, H. Effect of Orientation and Skylight Area Ratio on Building Energy Efficiency in the Qinghai–Tibet Plateau. *Buildings* **2024**, *14*, 755. https://doi.org/10.3390/buildings14030755

Academic Editor: Rafik Belarbi

Received: 17 February 2024
Revised: 4 March 2024
Accepted: 8 March 2024
Published: 11 March 2024

1. Introduction

As the global energy crisis intensifies and environmental issues become more severe, Carbon Neutrality and Carbon Peak have become a common focus of attention for the international community. The building sector is one of the largest energy-consuming industries in terms of total energy consumption [1], and its proportion is increasing yearly [2,3]. According to statistics [2], from 2005 to 2018, the energy consumption of the entire lifecycle of buildings in China rose from 934 million tons of coal equivalent (tce) in 2005 to 2.147 billion tce in 2018, with an average annual growth of 6.6%. In 2018, the lifecycle energy consumption of buildings accounted for 46.5% of total energy consumption [2]. Therefore, building energy efficiency is significant for carbon reduction and global sustainable development [4,5].

The Qinghai–Tibet Plateau, known as the "Water Tower of Asia", is the source of several major rivers in Asia [6]. However, with an average altitude of over 4000 m and low

average annual temperatures, the region has a prolonged heating period and high energy consumption for heating [7,8]. The traditional fossil fuel heating methods pose challenges to the region's ecological environment and water resource security. Located in the mid to low latitudes with high atmospheric transparency, the Qinghai–Tibet Plateau has abundant solar energy resources with tremendous potential for utilization [9]. Fully tapping into the region's rich solar energy resources can effectively reduce building energy consumption and decrease reliance on external traditional fossil fuels [10], promote green development, and accelerate progress towards the global dual-carbon goals.

During the design stage of a building, optimizing the building's orientation, structure, and layout can significantly enhance the thermal utilization efficiency of solar energy and reduce the building's heat load [11–13]. Orientation is an essential factor affecting building energy consumption [14]. Choosing the building orientation wisely can effectively increase the acquisition of solar energy for the building [15]. Skylights not only utilize natural light sources but also make use of solar radiation for indoor heating, which improves building energy efficiency [16]. The orientation of buildings and the use of skylights as highly effective and low-cost energy-saving strategies have attracted the attention of numerous researchers.

Numerous studies have demonstrated that optimizing building orientation can significantly reduce energy consumption [15]. In New Minia in Egypt, the difference in energy consumption between residential buildings' best and worst orientation can reach 7.5% [17]. In Iran, orienting a building to the south can reduce energy consumption by 11–39% [18]. In India, the optimal orientation of a building can save an additional 3.41% of energy compared with a reference building [19]. In China's hot summer and warm winter regions, the north–south orientation of residential buildings is 15% more energy-efficient than the east–west orientation [20]. Other studies also indicate that optimizing building orientation can reduce energy consumption by 20–36% [21,22]. In winter, the orientation of a building can significantly reduce its heating energy consumption [23], and an appropriate orientation can help reduce about 35% of a building's thermal losses during the winter season [24]. Regarding building energy consumption, the best orientation varies with geographical location and climatic conditions [25]. In the UK, the optimal residential orientation is south, while the least efficient is northwest [26]. The best building orientation is northward, and the worst is southward, in New Minia, Egypt [17]. In the Shandong region of China, the optimal range for building orientation is south to 15° south by east [27].

In addition to building orientation, skylight design is a critical factor in optimizing the use of solar energy [28]. As atriums serve as hubs connecting indoor and outdoor spaces, skylights are an essential part of their envelope structures [16,29]. In cold regions, large skylights can introduce solar radiation to reduce the heat load during the day [30], but they may also lead to significant heat loss at night due to poor thermal performance [31]. The area ratio (AR), which is the ratio of skylight area to roof area, is an important parameter affecting the thermal performance of buildings [32,33], and determining the appropriate skylight area is crucial for ensuring thermal comfort in atriums. Simulation studies on energy consumption indicate that reducing the skylight area can improve the thermal environment [34], achieving optimal daylighting and thermal comfort conditions when the AR is 1/4 [35]. However, other studies suggest increasing the area ratio can improve daylighting performance [36]. Furthermore, the skylight area-to-floor area ratio also significantly affects building energy consumption. When the skylight-to-floor area ratio is between 5.5% and 6%, it can reduce energy demand by 19% [28].

These studies above demonstrate clearly that orientation and AR have significant and complex impacts on building energy consumption. Especially in the Qinghai–Tibet Plateau region, characterized by unique geographical conditions and severe climate, the research field regarding building orientation and the skylight area ratio has not been sufficiently explored, which suggests a clear research void in this region. The Qinghai–Tibet plateau is the world's most extensive plateau with abundant solar thermal resources and is home to nearly ten million people with a strong demand for building heating. Exploring the

effect of orientation and AR on building energy consumption in this region has significant practical value. This article takes the comprehensive building of the Beiluhe Station on the Qinghai–Tibet plateau as the research subject. It validates the applicability of the EnergyPlus 9.4 software based on monitoring data. It simulates the heat load of buildings at different orientations from 90° (due east) to 270° (due west), as well as the heat load and room temperature under skylights with different ARs, providing reasonable building orientation and skylight AR for the region. This research can support the energy-saving design of buildings in the Qinghai–Tibet plateau and similar cold regions.

2. Overview of the Study Region

2.1. Study Subject

This paper selects the comprehensive building of the Beiluhe Station in the hinterland of the Source Region of the Yangtze River, Yellow River, and Lancang River on the Tibetan Plateau as the research subject. The station is located at 34°51′ N and 92°56′ E, with an altitude of 4628 m. The annual average temperature is −3.1 °C, and it is classified as a severe cold A zone according to the "Standard of Climatic Regionalization for Architecture" [37]. The building was constructed in 2017. It is a two-story ventilated concrete frame structure with a floor height of 3.3 m and covers an area of 631.24 m^2, with a shape coefficient of 0.31. The building is oriented due south, and at its center is an atrium covering 137.45 m^2. The total roof area is 650.67 m^2, and the southern slope of the roof has a skylight covering 316.73 m^2, resulting in an AR of 48.68%. The building's exterior wall facades are equipped with windows configured differently, with the window-to-wall ratios of each facade listed in Table 1 and the building's floor plan presented in Figure 1.

Table 1. Window-to-wall ratio.

	Total	North	East	South	West
Total Wall Area (m^2)	734.36	242.22	124.96	242.22	124.96
Window Area (m^2)	84.64	6.60	0.90	76.24	0.90
Overall Window-to-Wall Ratio (%)	11.53	2.72	0.72	31.28	0.72

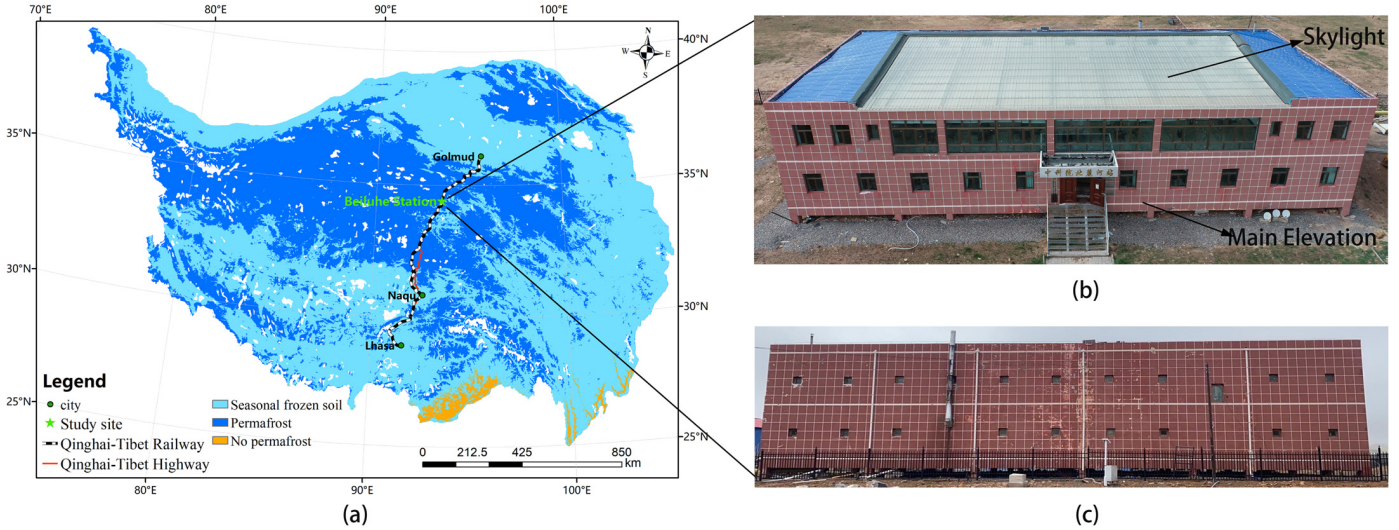

Figure 1. (**a**) Location of the study site; (**b**) main elevation of the building; (**c**) back elevation of the building.

2.2. Monitoring Method

Temperature and humidity sensors were installed in typical rooms within the building. The model of the sensors is RC-4HC, produced by Jiangsu Jingchuang Electric Co., Ltd. in Xuzhou, Jiangsu, China. The recording interval is 1 h, the accuracy of temperature recording

is ±0.5 °C, and the resolution is 0.1 °C. The sensors are mounted on brackets fixed to the wall 3 m above the ground. A layout diagram of the building's internal monitoring setup and a schematic of the monitoring equipment are shown in Figure 2.

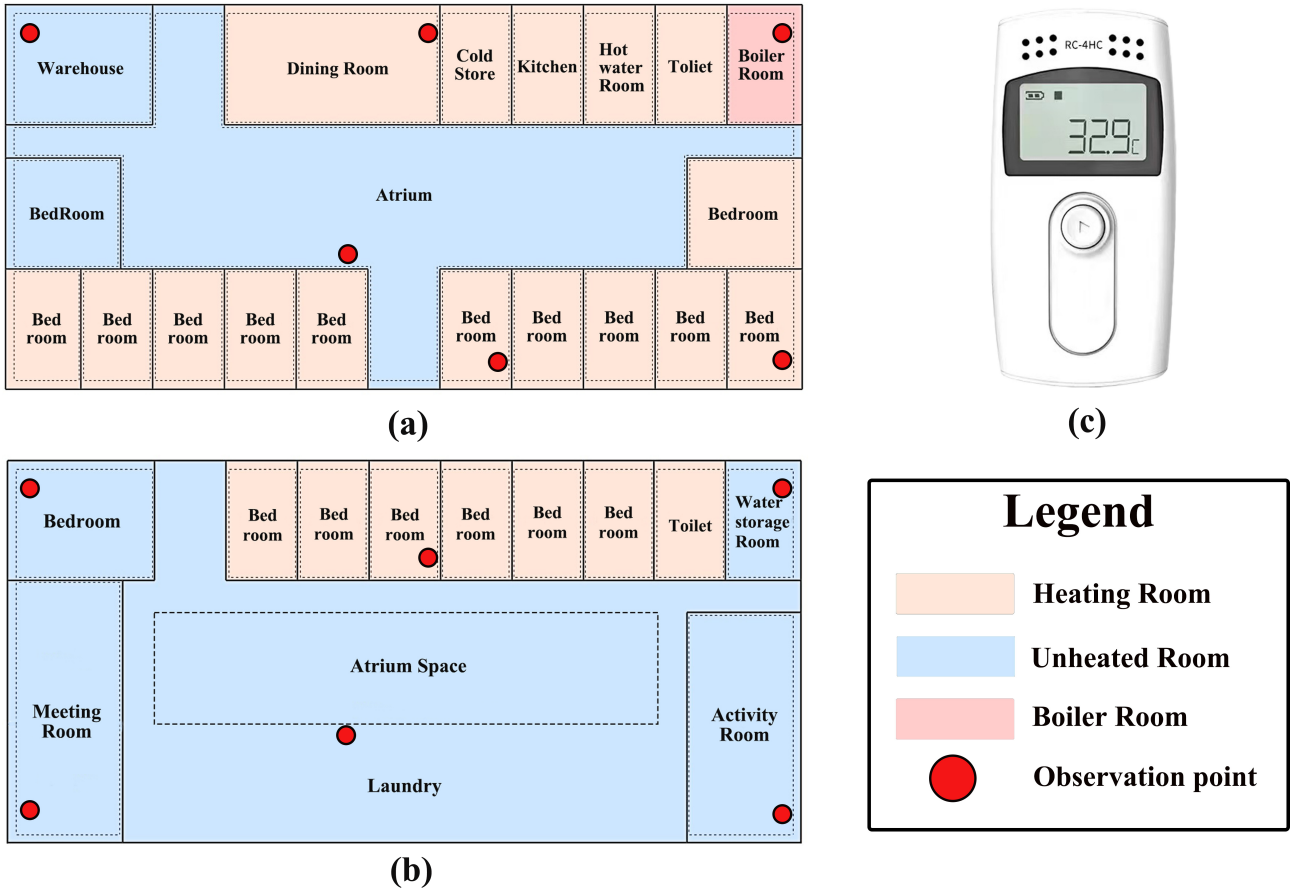

Figure 2. Room function, heating conditions, and monitoring point locations. (**a**) First floor; (**b**) second floor; (**c**) monitoring equipment.

In addition, a weather station is located 200 m west of the building to monitor the meteorological conditions of the region. The weather station has sensors for temperature and humidity, atmospheric pressure, four-component radiation, wind direction, and wind speed.

2.3. Local Climate Characteristics

Figure 3 displays the temperature distribution, radiation distribution, and wind frequency diagrams around the Beiluhe Station on the Qinghai–Tibet Plateau. The average annual temperature at Beiluhe Station is −3.1 °C, with monthly average temperatures below 0 °C for seven months. The coldest month is January, with an average monthly temperature of −14.32 °C, while the warmest month is July, with an average monthly temperature of 7.31 °C. According to the observational data, the maximum solar irradiance is 1155.00 Wh/m^2. The average solar radiation before noon, at 12 p.m. local time, is 37.8% higher than in the afternoon. The wind frequency diagram indicates that the prevailing winds in the region are from the west, with maximum wind speeds reaching up to 20 m/s.

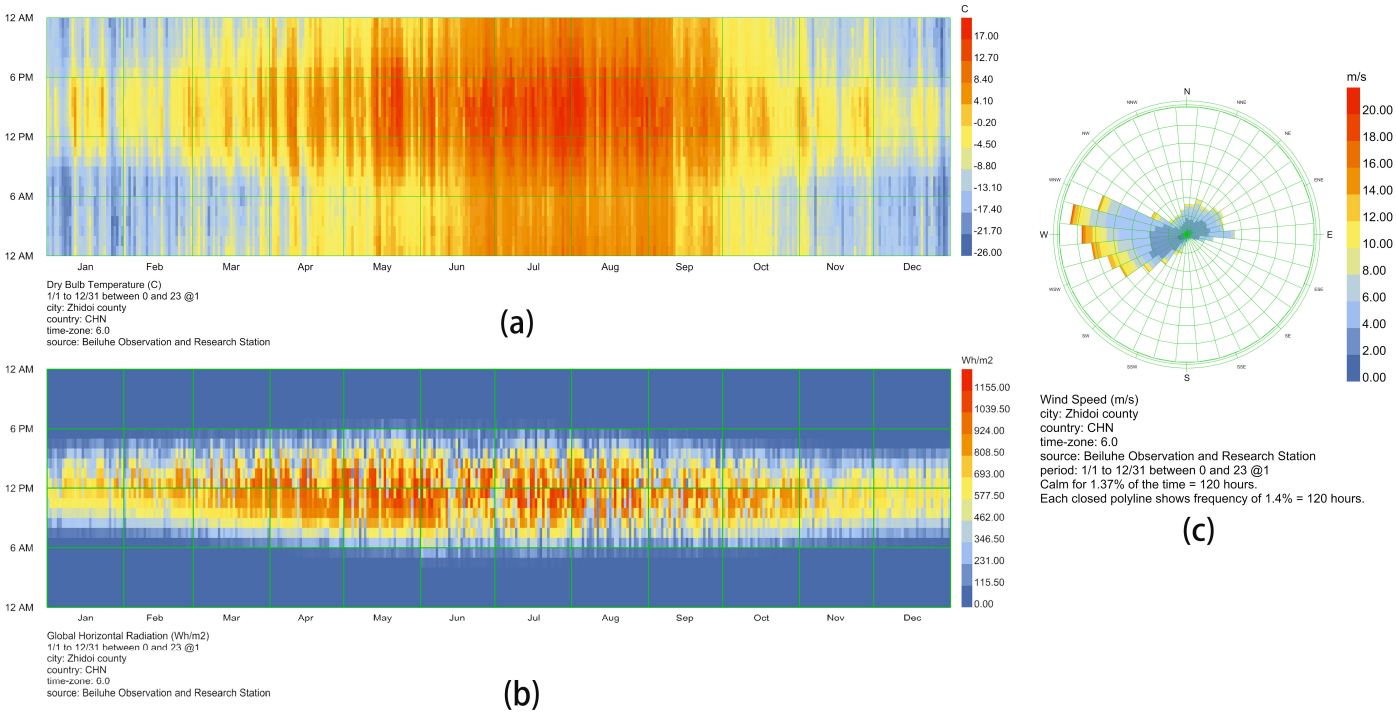

Figure 3. (**a**) Annual temperature distribution graph; (**b**) total radiation distribution graph; (**c**) wind frequency graph.

3. Study Methods

3.1. Energy Consumption Simulation Process

3.1.1. Simulation Software

The software EnergyPlus 9.4 used in this paper was co-developed by the U.S. Department of Energy and Lawrence Berkeley National Laboratory. It is widely used in building design and research and can perform comprehensive energy consumption simulation and analysis for heating, cooling, lighting, ventilation, and other energy uses in buildings [38]. EnergyPlus is recognized by numerous institutions and enterprises worldwide; hence, its simulation results are widely accepted.

3.1.2. Meteorological Data

The meteorological data mainly comes from the Beiluhe Meteorological Station. The separation of the total radiation into direct and diffuse radiation using the Gompertz function method [39], as shown in Equations (1) and (2).

$$K_n = A_1 A_2^{A_3 A_2^{-A_4 K_t}} \quad (1)$$

In the formula:

$$\begin{aligned} A_1 &= -0.1556 \sin^2 h + 0.1028 \sin h + 0.3748 \\ A_2 &= 0.7973 \sin^2 h + 0.1509 \sin h + 3.035 \\ A_3 &= 5.4307 \sin h + 7.2182 \\ A_4 &= 2.990 \\ K_t &= \frac{E}{E_0} \end{aligned} \quad (2)$$

In the formula, E represents the solar irradiance on the surface of the earth, E_0 corresponds to solar irradiance outside the atmosphere on a horizontal plane, and h denotes the solar altitude angle, and the calculation formulas for E, E_0, h, and local time, etc., can be found in the literature [40,41].

3.1.3. Setting of Building Envelope and Thermal Parameters

The construction of each building envelope structure and the thermal parameters are shown in Tables 2 and 3. The thermal parameters are derived from the Chinese standard "Thermal Design Code for Civil Buildings" [42], and the data for transparent envelope structures come from the International Glass Database (IGDB) [43]. This model is also based on these fixed settings.

Table 2. Building envelope details and thermal parameters.

Building Envelope	Construction	Heat Conductivity (W/m·K) [42]	Thickness (m)	Heat-Transfer Coefficient (W/m^2·K)
Exterior wall	Cement mortar	0.930	0.005	0.230
	Cement lime plaster mortar	0.870	0.011	
	Autoclaved aerated concrete block	0.140	0.300	
	XPS insulation board	0.030	0.060	
	Cement mortar	0.930	0.018	
Interior wall	Cement mortar	0.930	0.005	0.580
	Cement lime plaster mortar	0.870	0.011	
	Autoclaved aerated concrete block	0.140	0.200	
	Cement lime plaster mortar	0.870	0.011	
	Cement mortar	0.930	0.005	
External floor	Cement mortar	0.930	0.020	0.221
	Reinforced concrete slab	1.740	0.200	
	Polyurethane rigid foam	0.024	0.100	
	Cement mortar	0.930	0.020	
Internal floor	Reinforced concrete slab	1.740	0.200	2.460
	Cement mortar	0.930	0.010	
Roof	SBS sheet	0.170	0.008	0.776
	Cement mortar	0.930	0.025	
	Coal ash	0.230	0.080	
	Cement cinder	0.760	0.510	
	Reinforced concrete slab	1.740	0.120	

Table 3. Thermal performances of skylight and external window.

Building Envelope	Construction	Solar Heat Gain Coefficient	Heat-Transfer Coefficient (W/m^2·K)
External window	Insulating glass (6 + 12A + 6)	0.749	2.695
Skylight	PC board	0.701	2.014

3.1.4. HVAC System

The heating control temperature is set at 18 °C (24 h), with a startup temperature of 12 °C, and the heating period extends from January to June and from August to December. The lighting power density is 5 W/m^2, and the equipment power density is 3.8 W/m^2. The operation schedules for lighting, equipment, and personnel occupancy are detailed in the referenced literature [44].

3.1.5. Model Validation

This paper verifies the model by comparing the temperature data obtained from the atrium measurements with the data obtained from simulations, using the correlation coefficient (R^2) to evaluate the model's accuracy. The larger the R^2 value, the closer the

simulation values are to the observed values. The formula for calculating the evaluation index is as shown in Equation (3):

$$R^2 = 1 - \sum_{i=1}^{n} (O_i - S_i)^2 / \sum_{i=1}^{n} (O - \overline{O})^2 \quad (3)$$

In the formula, O_i, S_i represent the observed and simulated values, respectively, and $\overline{O}$ is the average of the observed values.

Figure 4 displays the comparison between the simulated values and the monitored values of the atrium temperature, with an R^2 value of 0.954. The simulation curve slightly differs from the curve of the observed values, but, overall, the trends are consistent. The reasons for the simulation error include discrepancies between the actual thermal properties of the building envelope materials and their parameters in the model. There are also errors in the process of separating direct and diffuse radiation. The comparative analysis of the simulation and measurement values indicates that the temperature simulation results of the EnergyPlus 9.4 software for the object of this study are accurate.

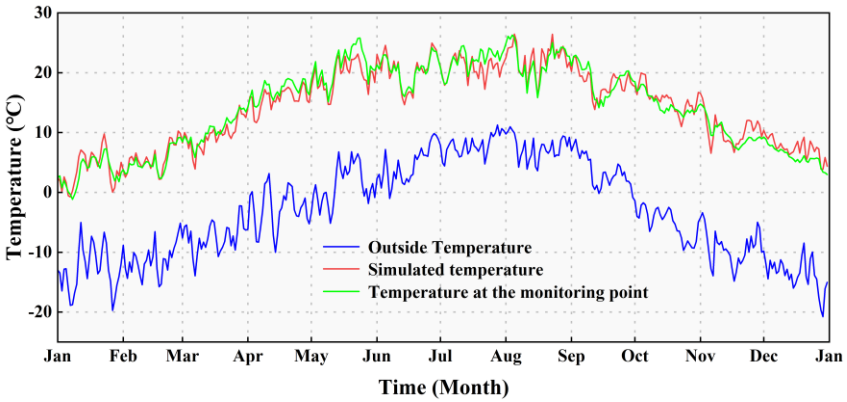

Figure 4. Comparison between simulated and measured values of atrium temperature.

The heating coal for Beiluhe Station comes from the Mulei Coal Mine in Xinjiang, with an ash content of 3.83% and a calorific value of 23.97 MJ/kg, classified as Class II anthracite. Per the "specification for small type boilers and atmospheric hot water boilers" [45], the boiler's thermal efficiency is 60%. According to the "general principles for the calculation of the comprehensive energy consumption" [46], the comprehensive energy consumption is calculated using formula (4), and the verification of energy consumption uses formula (5) for determination.

$$E = \sum_{i=1}^{n} (E_i \times k_i) \quad (4)$$

In the formula, E represents the comprehensive energy consumption, n represents the number of types of energy consumed, E_i represents the quantity of the i type of energy actually consumed during production or service processes, and k_i represents the standard coal conversion coefficient for the i type of energy.

$$ERR_{month} = \left[\frac{(M - S)_{month}}{M_{month}} \right] \times 100\% \quad (5)$$

In the formula, ERR_{month} represents the monthly error between the simulated and actual energy consumption, M represents the actual measured value of energy consumption, and S represents the simulated value of energy consumption.

Through the analysis of meteorological data, December and January are identified as the coldest months of the year. Based on the survey of coal usage at Beiluhe Station during this period, the average daily coal consumption is about 70 kg. Hence, December

and January are selected as the key verification months for assessing heating energy consumption. According to the "general principles for the calculation of the comprehensive energy consumption" [46], the conversion coefficient for thermal value to standard coal is 0.03412 kgce/MJ for anthracite, and 0.82 kgce/MJ for smokeless coal. Through simulation, the heating amounts for December and January are 8149.92 kW·h and 9226.57 kW·h, respectively. Converting these amounts to kilograms of standard coal equivalent (kgce) using formula (4), they are 1001.07 kgce and 1133.32 kgce, respectively. Ignoring the thermal loss from the heating system's pipeline network, the actual heating amounts for December and January are 1067.64 kgce. Comparing the actual energy consumption with the simulated values, the deviations for December and January are 6.65% and −6.15%, respectively. According to the "technical code for the retrofitting of public building on energy efficiency" [47], a deviation between calculations and simulations within ±15% is an acceptable error range. Therefore, the energy consumption data simulated by the EnergyPlus 9.4 software are accurate and reliable.

Based on the dual verification of temperature and energy consumption, EnergyPlus 9.4 software can be used for the analysis of energy consumption and temperature at the comprehensive building of Beiluhe station.

3.2. Operation Setting

As shown in Figure 5. This paper defines north as 0°, increasing clockwise by 15° increments from 90° (east) to 270° (west), and uses EnergyPlus 9.4 software to simulate heat loads for 13 different orientations, as well as the heat load and atrium temperature under various ARs.

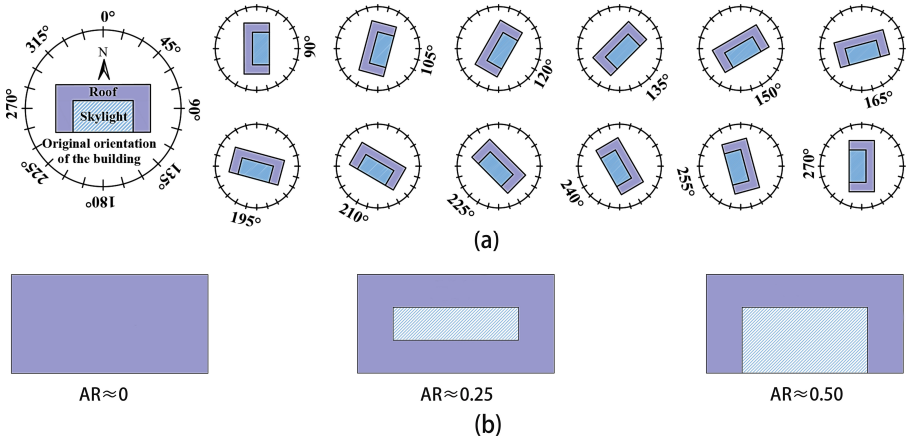

Figure 5. Simulation method. (**a**) Orientation; (**b**) area ratio.

4. Simulation Results and Analysis

4.1. Analysis of Heat Load Energy Saving for Different Building Orientations

Figure 6 shows the variation curve of the annual total heat load of a building under different orientations. As shown in Figure 6, the overall annual heat load presents a parabolic shape that opens upward, showing a trend of decreasing first and then increasing. Specifically, from 90° to 150°, the heat load decreases. Starting from the 150° orientation, the heat load begins to rise until it reaches 180°. This is because the general weather pattern of cloud cover changes in the plateau region: there is less stable cloud cover in the morning, and it increases rapidly in the afternoon [48–50]. Cloud cover blocks the solar radiation reaching the ground, leading to the asymmetry in the diurnal variation of total solar radiation on the plateau, with higher levels in the morning and lower in the afternoon [51]. This result is consistent with the radiation data measured by the Beiluhe weather station. Therefore, when the building's orientation is between 90° and 270°, under the condition that the absolute value of the angle difference between the building's orientation and the due south direction is the same, the main facade and the skylight of the building facing

southeast receive more solar radiation than those facing southwest. The influence of wind on the primary facade orientation is minor within this range (Figure 2).

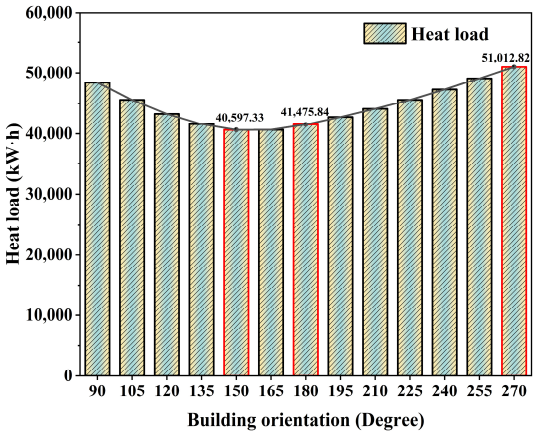

Figure 6. Changes in annual heat load of building under different orientations.

At 150°, the building's heat load is the smallest, at 40,597.33 kWh, which is an energy savings of 2.12% compared with the current actual orientation (180°) of the Beiluhe Station comprehensive building. The maximum heat load occurs at 270°, at 51,012.82 kWh, which is 22.99% higher than the energy consumption of the current actual orientation (180°). The difference in heat load between the two is 25.66%. To further clarify the relationship between orientation and heat load, a study was conducted on the monthly values of building heat load.

Figure 7 shows the variation in building heat load from January to December under different orientations. As depicted, with the progression of months, the overall heat load for each orientation exhibits a parabola shape that opens upward, showing a trend of decreasing first and then increasing. This is due to the change in outdoor temperature affecting the building's heating demand. From January to June, the outdoor temperature gradually increases, leading to a decrease in heat load. The outdoor temperature gradually decreases from August to December, and the heat load increases accordingly. From January to March and August to December, the heat loads are lower between 135° and 180°. These months belong to the colder seasons, and due to the strong diurnal variation characteristics of solar radiation in the Qinghai–Tibet Plateau region, the solar radiation within the range of 135° to 180° contributes more to the building's heat gain, reducing the heating requirements of the building.

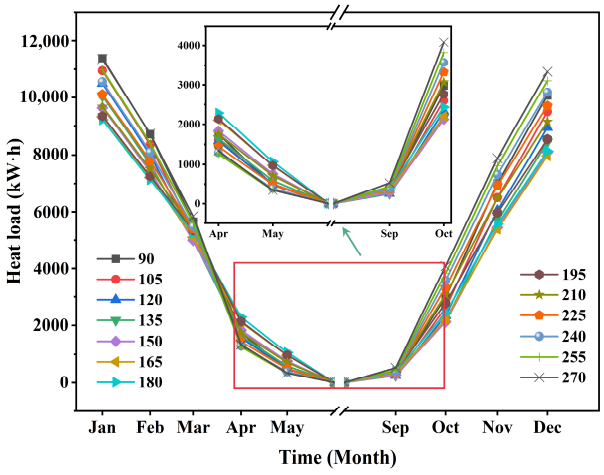

Figure 7. Monthly variation curve of building heat load.

In plateau regions, where temperatures are relatively low throughout the four seasons, maintaining indoor temperatures requires significant energy. Observing the variation curve of building heat loads from January to December, it can be seen that the heat load between 135° and 180° remains at a lower level for most of the year. Considering the annual total heat load of the building, the heat load at 150° is the lowest.

4.2. Analysis of Heat Load with Varied Skylight Areas

Figure 8 presents the annual total thermal load of buildings with different ARs at a 150° orientation, demonstrating significant variations in heat load with different skylight areas. When the AR is 0, the building's heat load is the highest at 50,535.93 kW·h; with an AR of 0.25, the heat load decreases to 44,619.69 kW·h; and the smallest heat load is found at an AR of 0.5, with 40,597.32 kW·h. This indicates that the heat load is inversely correlated with the area of the skylight. That is, the larger the skylight area, the smaller the building's heat load. Adopting skylights in building roofs on the plateau can significantly save energy. With an AR of 0.5, there is an energy saving of 19.67% compared with buildings with an AR of 0. The larger the skylight area, the more solar radiation enters the atrium. After the sun's short-wave radiation enters the atrium through the skylight, the indoor temperature rises, and the skylight blocks the long-wave radiation emitted from the atrium, reducing energy release and thus leading to an increase in atrium temperature [52]. Meanwhile, the existence of the atrium's buffering effect [53] also avoids direct contact of the surrounding rooms with the external environment, creating a suitable daytime activity space for personnel at workstations, while also providing auxiliary heating to surrounding rooms.

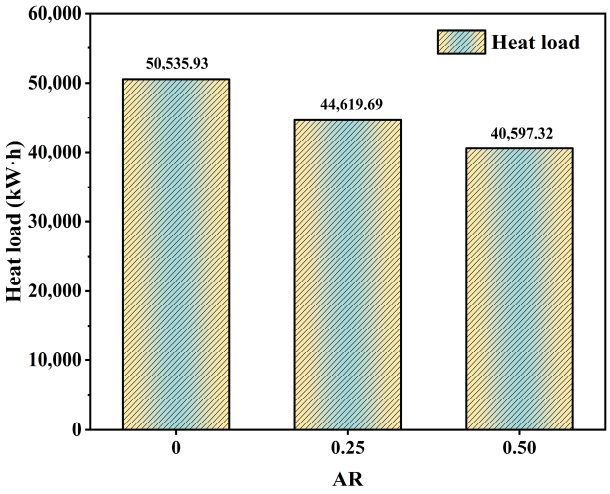

Figure 8. Building heat load diagram with different AR under 150° orientation.

Figure 9 depicts the skylight heat gains and the curve for solar radiation entering indoors through the skylight at a 150° orientation with different ARs. The graph shows that the heat losses through the skylight and the solar radiation energy entering indoors positively correlate with the AR. During the summer months of June, July, and August, skylights contribute significant heat gains to the interior regardless of AR, peaking in July. In March, April, May, and September, the solar radiation introduced by the skylight far exceeds its heat losses, and this difference becomes more pronounced as the AR increases. This indicates that more enormous skylights in these seasons can more effectively utilize solar radiation to provide heat indoors. In winter, more enormous skylights can lead to more significant heat loss through the skylight. However, the heat losses can be partially or entirely offset by the solar radiation energy they introduce, reducing or eliminating the building's reliance on traditional heating systems and lowering energy consumption.

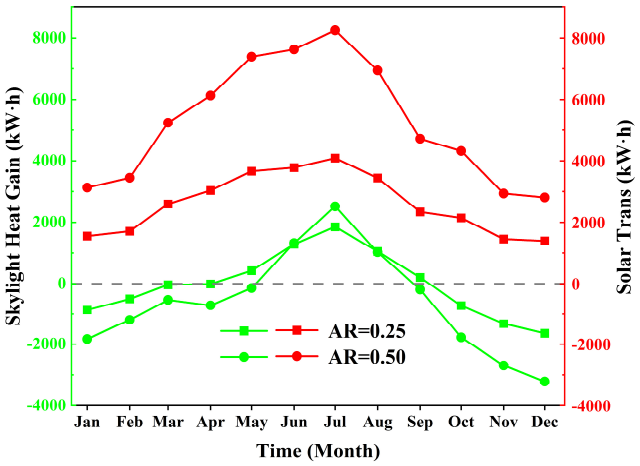

Figure 9. Skylight heat gain and solar radiation curves for skylight with different ARs under 150° orientation.

4.3. Indoor Temperature Analysis under Different Skylight Areas

Skylights can effectively utilize daytime solar radiation to improve the indoor thermal environment, but due to their poor thermal performance, there are significant heat losses at night. The solar radiation received by the skylight directly affects the atrium, and since the warehouse is less affected by external disturbances compared with other rooms, it can serve as an indicator of how changes in the skylight area influence temperature variations in other rooms. Figure 10 shows the daily temperature variation curves for the atrium and warehouse under different ARs at a 150° orientation. From the graph, it is evident that for both the warehouse and the atrium, the overall trend of the temperature curves is consistent across the three ARs, with larger ARs resulting in more pronounced temperature fluctuations. The temperature positively correlates with the AR for the atrium and warehouse from March to October. From November to February of the following year, whether for warehouses or atriums, the temperature difference under the three area ratios is not significant. During this period, the skylight maintains a balance between the energy gained during the day and the energy lost at night.

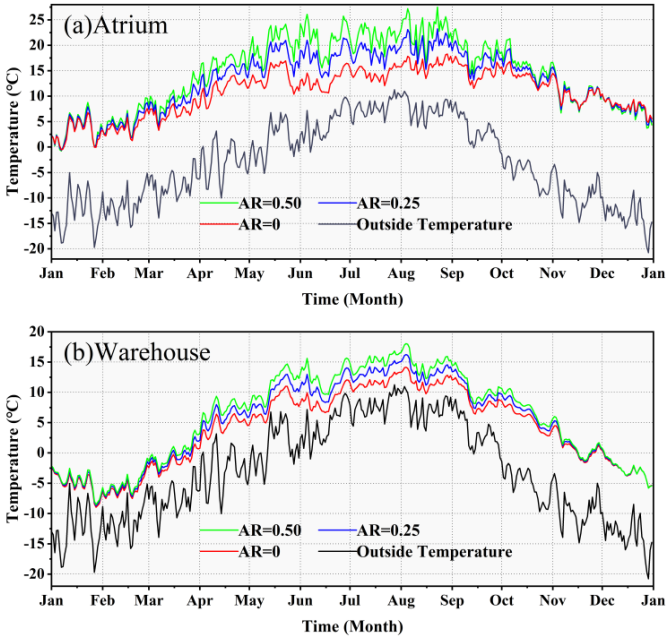

Figure 10. Daily average temperature curve of atrium and warehouse with different ARs under 150° orientation.

5. Discussions

5.1. Optimal Building Orientation in the Qinghai–Tibet Plateau Region

This paper utilized EnergyPlus 9.4 software and relied on actual meteorological data to explore the impact of building orientation on heat load in the cold region of the Qinghai–Tibet Plateau. The results show that building orientation significantly impacts the heat load in this region. However, the optimal orientation differs from previous studies, with 150° (30° south by east) being the orientation with the smallest heat load, and the heat loads between orientations of 135° to 180° differing very minimally (Figure 7).

Building energy consumption exhibits differences in heating or cooling demand under varying climatic conditions. In regions with high cooling energy demands, building orientations that reduce solar radiation are preferred, such as the best orientation for Bandung in Indonesia, which is south of the equator, being southwest [54], while for New Minia in Egypt, which is north of the equator, the orientation is towards the north [17]. For the Iranian Plateau, which is at a similar latitude to the Tibetan Plateau, there is a need for heating in the winter. However, due to the relatively arid climate of the region, the difference in radiation between morning and afternoon is small, making a southward orientation optimal for buildings in this area [18].

The optimal orientation for the comprehensive building of Beiluhe Station is skewed towards the east. This result aligns with the radiation mechanism of the Yin–Yang slope along the Qinghai–Tibet Railway, where solar radiation on the plateau is stronger in the morning than in the afternoon. For the north–south Qinghai–Tibet line, the morning solar radiation primarily affects the eastern slope, while the afternoon solar radiation primarily affects the western slope [50]. Therefore, the eastern slope inevitably receives more solar radiation than the western slope [50]. Thus, for buildings in the Qinghai–Tibet Plateau region, an eastward orientation allows them to receive more solar radiation. As Morrissey has pointed out, buildings with many windows on their façades usually benefit from higher levels of solar radiation inside [55], which can even replace air conditioning systems in high solar radiation areas, like the Qinghai–Tibet Plateau during winter [10]. The main façade of the comprehensive building of Beiluhe Station has a large window-to-wall ratio and a large skylight on the roof. Given the strong total solar radiation in the region and the particularly intense solar radiation in the morning, this leads to the best orientation range being between 135° (45° south by east) to 180° (due south).

5.2. The Impact of Varied ARs on Heat Load

The simulation results presented in this paper indicate that, as the skylight AR increased from 0 to 0.25 and 0.50, the heating load of the building decreased by 11.71% and 19.67%, respectively (Figure 8). Studies in Austin and Boston suggest that heat load would increase regardless of the variation in skylight area ratio [56,57].

Austin and Boston, being low-altitude regions with less winter solar radiation, found that the positive impact of solar radiation indoors cannot offset the negative effect of heat dissipation through skylights. Hence, any skylight area can increase the thermal load in these regions [56,57]. However, for the Qinghai–Tibet Plateau region, the intense winter solar radiation can partially or completely compensate for the energy loss through skylights (Figure 9). Consequently, the skylight of the Beiluhe Station's comprehensive building still plays a significant role in the warming effect during winter.

Skylight introduces solar radiation indoors, which is a beneficial factor for reducing energy consumption in the frigid winter months. For low-altitude regions with cold winters and hot summers, skylights increase the demand for cooling energy in summer [30,58]. However, in the Source Region of the Yangtze River, Yellow River, and Lancang River on the Qinghai–Tibet Plateau, the average temperature during the warmest month in summer is below 10 °C. According to China's "Indoor Air Quality Standards" [59], heating is mandatory for buildings when the temperature falls below 16 °C. Hence, even the summer season requires heating in this region. Under such climatic conditions, buildings in the region have year-round heating demands. Solar radiation entering indoors will

only positively impact the indoor thermal environment and will not cause overheating in summer (Figure 11). An overall analysis for both winter and summer suggests that skylight design in the Qinghai–Tibet Plateau region can reduce the building's annual energy consumption.

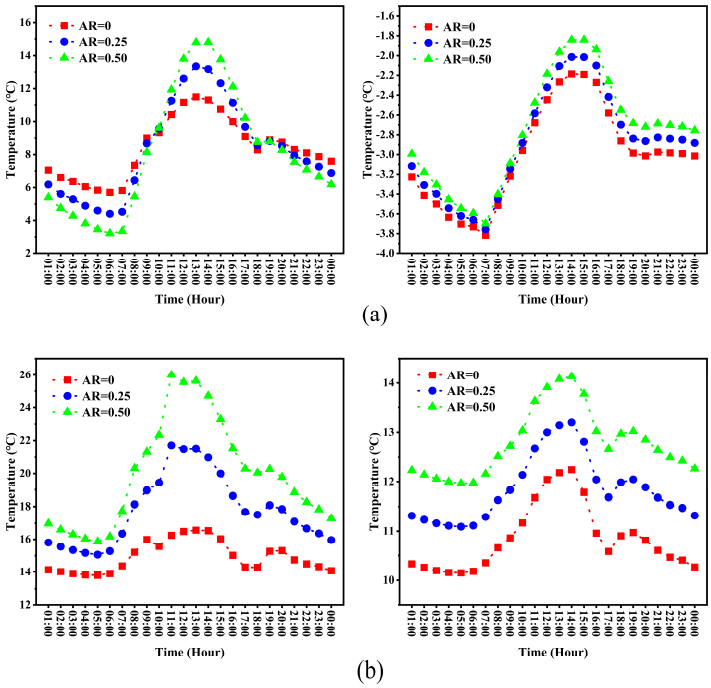

Figure 11. (**a**) Temperature of atrium and warehouse on the winter solstice facing 150; (**b**) temperature of atrium and warehouse at 150 towards the lower summer solstice.

While skylight can reduce the heating load of buildings on the Qinghai–Tibet Plateau, the energy savings are only 9.01% when the skylight AR increases from 0.25 to 0.50, which is less than the decrease from 0 to 0.25. This indicates no linear negative correlation between the heating heat load and the skylight area ratio in the Qinghai–Tibet Plateau region. Once the skylight area ratio reaches a certain threshold, the rate of decline in the building's heat load will slow down or even stabilize.

6. Conclusions

This paper takes the comprehensive building of Beiluhe Station in the Source Region of the Yangtze River, Yellow River, and Lancang River, located in the hinterland of the Qinghai–Tibet Plateau, as a case study. Based on monitoring and simulation results, the paper discusses the impact of building orientation and the area ratio of skylights on the heating energy consumption of buildings in the Qinghai–Tibet Plateau area and draws the following conclusions:

(a) In regions with intense solar radiation like the Qinghai–Tibet Plateau, the orientation and design of skylights significantly affect the building's energy efficiency and the quality of the indoor environment.

(b) For the building style discussed in this paper, the optimal orientation of the building is 30° south by east, with the best orientation ranging from 45° south by east to due south.

(c) The skylight design optimization can reduce buildings' annual energy consumption in the Qinghai–Tibet Plateau region. There is a negative correlation between the building's heat load and the area ratio of the skylight. When the area ratio of the skylight reaches a certain value, the rate of decline in building heat load will slow down or even tend to stabilize.

The conclusions of this paper can provide valuable guidance for the architectural design and construction in the Qinghai–Tibet Plateau region, especially when considering the orientation of buildings and the area of skylights. It is recommended that future design practices take these factors into comprehensive consideration to enhance the energy efficiency of buildings and the comfort of occupants. This paper provides empirical support for maximizing building energy efficiency in the region and offers valuable references for architectural professionals in designing for similar geographic and climatic conditions. Future research will focus on the optimal window-to-wall ratio for the external fenestration of building envelopes in the Qinghai–Tibet Plateau region. The expansion of this research is expected to further improve the buildings' ability to harness solar radiation and contribute to the development of more refined design solutions that can adapt to the constantly changing climate conditions.

Author Contributions: Conceptualization, Y.W. (Yingmei Wang); Methodology, H.Q., S.Z. and H.S.; Software, Y.W. (Yingmei Wang); Validation, Y.W. (Yingmei Wang), H.Q. and J.C.; Formal Analysis, H.Q. and Y.W. (Yan Wang); Investigation, Y.W. (Yan Wang), X.H. and P.R.; Resources, Y.W. (Yingmei Wang) and J.C.; Data Curation, H.Q.; Writing—Original Draft, H.Q.; Writing—Review and Editing, Y.W. (Yingmei Wang); Visualization, X.H. and P.R.; Supervision, Y.W. (Yingmei Wang); Project Administration, S.Z. and H.S.; Funding Acquisition, Y.W. (Yingmei Wang) and J.C. All authors have read and agreed to the published version of the manuscript.

Funding: This research was supported by the National Key Research and Development Program of China (2022YFF1302600), the State Key Laboratory of Frozen Soil Engineering Funds (SKLFSE-ZY-19), and the program of the Research and Development of Science and Technology of China State Railway Group Co., Ltd. (K2022G017).

Data Availability Statement: The original contributions presented in the study are included in the article, further inquiries can be directed to the corresponding author.

Conflicts of Interest: Author Shouhong Zhang was employed by the company China Railway Qinghai-Tibet Group Co., Ltd. Author Hanyu Song was employed by the company Shangqiu Branch of China Tower Co., Ltd. The remaining authors declare that the research was conducted in the absence of any commercial or financial relationships that could be construed as a potential conflict of interest.

Abbreviations

AR	area ratio
ARs	area ratios
IGDB	International Glass Database

References

1. Conti, J.; Holtberg, P.; Diefenderfer, J.; LaRose, A.; Turnure, J.T.; Westfall, L. *International Energy Outlook 2016 with Projections to 2040*; USDOE Energy Information Administration (EIA): Washington, DC, USA, 2016.
2. China Association of Building Energy Efficiency. China Building Energy Consumption Annual Report 2020. *J. Build. Energy Effic.* **2021**, *49*, 1–6. (In Chinese)
3. Jiang, Y. Current building energy consumption in china and effective energy efficiency measures. *Heat. Vent. Air Cond.* **2005**, *35*, 30–40. (In Chinese) [CrossRef]
4. Fang, Y.; Cho, S. Design optimization of building geometry and fenestration for daylighting and energy performance. *Solar Energy* **2019**, *191*, 7–18. [CrossRef]
5. Mirrahimi, S.; Mohamed, M.F.; Haw, L.C.; Ibrahim, N.L.N.; Yusoff, W.F.M.; Aflaki, A. The effect of building envelope on the thermal comfort and energy saving for high-rise buildings in hot–humid climate. *Renew. Sustain. Energy Rev.* **2016**, *53*, 1508–1519. [CrossRef]
6. Yao, T.; Bolch, T.; Chen, D.; Gao, J.; Immerzeel, W.; Piao, S.; Su, F.; Thompson, L.; Wada, Y.; Wang, L. The imbalance of the Asian water tower. *Nat. Rev. Earth Environ.* **2022**, *3*, 618–632. [CrossRef]
7. Yihao, L. Improve the Indoor Thermal Environment of Alpine Region Building Technical Measures and Research in Tibet. Master's Thesis, Southwest Jiaotong University, Chengdu, China, 2012. (In Chinese)
8. Wang, M. Study on Indoor Thermal Environment of Buildings in Cold Plateau Area. Master's Thesis, Chongqing University, Chongqing, China, 2019. (In Chinese)

9. Wang, Q.; Qiu, H.-N. Situation and outlook of solar energy utilization in Tibet, China. *Renew. Sustain. Energy Rev.* **2009**, *13*, 2181–2186. [CrossRef]
10. Gong, X.; Akashi, Y.; Sumiyoshi, D. Optimization of passive design measures for residential buildings in different Chinese areas. *Build. Environ.* **2012**, *58*, 46–57. [CrossRef]
11. Baharvand, M.; Ahmad, M.H.B.; Safikhan, T.; Mirmomtaz, S.M.M. Thermal performance of tropical atrium. *Environ. Clim. Technol.* **2013**, *12*, 34–40. [CrossRef]
12. Boukli Hacene, M.; Chabane Sari, N. Energy efficient design optimization of a bioclimatic house. *Indoor Built Environ.* **2020**, *29*, 270–285. [CrossRef]
13. Su, Y.; Zhao, Q.; Zhou, N. Improvement strategies for thermal comfort of a city block based on PET Simulation—A case study of Dalian, a cold-region city in China. *Energy Build.* **2022**, *261*, 111557. [CrossRef]
14. Wong, K.d.; Fan, Q. Building information modelling (BIM) for sustainable building design. *Facilities* **2013**, *31*, 138–157. [CrossRef]
15. Pacheco, R.; Ordóñez, J.; Martínez, G. Energy efficient design of building: A review. *Renew. Sustain. Energy Rev.* **2012**, *16*, 3559–3573. [CrossRef]
16. Acosta, I.; Varela, C.; Molina, J.F.; Navarro, J.; Sendra, J.J. Energy efficiency and lighting design in courtyards and atriums: A predictive method for daylight factors. *Appl. Energy* **2018**, *211*, 1216–1228. [CrossRef]
17. Elhadad, S.; Baranyai, B.; Gyergyák, J. The impact of building orientation on energy performance: A case study in new Minia, Egypt. *Pollack Period.* **2018**, *13*, 31–40. [CrossRef]
18. Kohansal, M.E.; Akaf, H.R.; Gholami, J.; Moshari, S. Investigating the simultaneous effects of building orientation and thermal insulation on heating and cooling loads in different climate zones. *Archit. Eng. Des. Manag.* **2022**, *18*, 410–433. [CrossRef]
19. Prasad, A.; Anchan, S.; Kamath, M.; Akella, V. Impact of building orientation on energy consumption in the design of green building. *Int. J. Emerg. Res. Manag. Technol.* **2017**, *6*, 2278–9359.
20. Hu, D.; Chen, D.; Shan, P.; Huang, F.; Huang, H. Influence of Residential Building Orientations to Energy Consumption in Hot Summer and Warm Winter Zone. *J. Build. Energy Effic.* **2017**, *45*, 57–60. (In Chinese) [CrossRef]
21. Spanos, I.; Simons, M.; Holmes, K.L. Cost savings by application of passive solar heating. *Struct. Surv.* **2005**, *23*, 111–130. [CrossRef]
22. Aksoy, U.T.; Inalli, M. Impacts of some building passive design parameters on heating demand for a cold region. *Build. Environ.* **2006**, *41*, 1742–1754. [CrossRef]
23. Albatayneh, A.; Alterman, D.; Page, A.; Moghtaderi, B. The significance of the orientation on the overall buildings thermal performance-case study in Australia. *Energy Procedia* **2018**, *152*, 372–377. [CrossRef]
24. Albatayneh, A.; Mohaidat, S.; Alkhazali, A.; Dalalah, Z.; Bdour, M. The influence of building's orientation on the overall thermal performance. *Environ. Sci. Sustain. Dev.* **2018**, *3*, 63–69. [CrossRef]
25. Ren, W.; Zhao, J.; Chang, M. Energy-saving optimization based on residential building orientation and shape with multifactor coupling in the Tibetan areas of western Sichuan, China. *J. Asian Archit. Build. Eng.* **2023**, *22*, 1476–1491. [CrossRef]
26. Abanda, F.; Byers, L. An investigation of the impact of building orientation on energy consumption in a domestic building using emerging BIM (Building Information Modelling). *Energy* **2016**, *97*, 517–527. [CrossRef]
27. Ji, W.; Wang, J.; Xie, Y. Influence of Dormitory Building Orientation on Energy Consumption in Cold Zones: Taking the Dormitory of Shandong Jianzhu University as an Example. *J. Build. Energy Effic.* **2022**, *50*, 34–41. (In Chinese) [CrossRef]
28. Motamedi, S.; Liedl, P. Integrative algorithm to optimize skylights considering fully impacts of daylight on energy. *Energy Build.* **2017**, *138*, 655–665. [CrossRef]
29. Liu, X. The Design of Atrium and Architectural Daylight Roof. Master's Thesis, Hebei University of Technology, Wuhan, China, 2006.
30. Yang, Y.; Wu, H.; Yang, L.; Xu, T.; Ding, Y.; Fu, P. Thermal and day-lighting performance of aerogel glazing system in large atrium building under cooling-dominant climates. *Energy Procedia* **2019**, *158*, 6347–6357. [CrossRef]
31. Sher, F.; Kawai, A.; Güleç, F.; Sadiq, H. Sustainable energy saving alternatives in small buildings. *Sustain. Energy Technol. Assess.* **2019**, *32*, 92–99. [CrossRef]
32. Sudan, M.; Mistrick, R.G.; Tiwari, G. Climate-Based Daylight Modeling (CBDM) for an atrium: An experimentally validated novel daylight performance. *Sol. Energy* **2017**, *158*, 559–571. [CrossRef]
33. Fan, Z.; Yang, Z.; Yang, L. Daylight performance assessment of atrium skylight with integrated semi-transparent photovoltaic for different climate zones in China. *Build. Environ.* **2021**, *190*, 107299. [CrossRef]
34. Wu, P.; Zhou, J.; Li, N. Influences of atrium geometry on the lighting and thermal environments in summer: CFD simulation based on-site measurements for validation. *Build. Environ.* **2021**, *197*, 107853. [CrossRef]
35. Nasrollahi, N.; Abdolahzadeh, S.; Litkohi, S. Appropriate geometrical ratio modeling of atrium for energy efficiency in office buildings. *J. Build. Perform.* **2015**, *6*, 95–104.
36. Li, J.; Ban, Q.; Chen, X.; Yao, J. Glazing sizing in large atrium buildings: A perspective of balancing daylight quantity and visual comfort. *Energies* **2019**, *12*, 701. [CrossRef]
37. *GB 50178-1993*; Standard of Climatic Regionalization for Architecture. Ministry of Construction of the People's Republic of China: Beijing, China, 1993.
38. Pan, Y. *Building Energy Simulation Handbook*; China Architecture & Building Press: Beijing, China, 2013; ISBN 9787112155101.

39. Zhang, Q.; Yang, H. *Manual of Standard Meteorological Data for Buildings*; China Architecture & Building Press: Beijing, China, 2012; ISBN 9787112137701.
40. Wang, B. Solar Radiation Calculation Lecture one: Calculation of Astronomical Parameters in Solar Energy. *Sol. Energy* **1999**, 8–10. (In Chinese)
41. Wang, B. Solar Radiation Calculation Lecture three: Calculation of Extraterrestrial Horizontal Radiation. *Sol. Energy* **1999**, 12–13. (In Chinese)
42. *GB 50176-2016*; Thermal Design Code for Civil Buildings. Ministry of Construction of the People's Republic of China: Beijing, China, 2016.
43. Available online: https://windows.lbl.gov/software/igdb (accessed on 18 December 2023).
44. *JGJ 26-2010*; Design Standard for Energy Efficiency of Residential Buildings in Severe Cold and Cold Zones. Ministry of Construction of the People's Republic of China: Beijing, China, 2010.
45. *JB/T 7985-2002*; Specification for Small Type Boilers and Atmospheric Hot Water Boilers. State Economic and Trade Commission of the People's Republic of China: Beijing, China, 2002.
46. *GB/T 2589-2020*; General Principles for the Calculation of the Comprehensive Energy Consumption. Energy Fundamentals and Management: Beijing, China, 2020.
47. *JGJ 176-2009*; Technical Code for the Retrofitting of public Building on Energy Efficiency. Ministry of Construction of the People's Republic of China: Beijing, China, 2009.
48. Ye, D.; Gao, Y. *Meteorology of the Qinghai—Tibet Plateau*; Science Press: Beijing, China, 1979; ISBN 130311072.
49. Zhang, J. *Advances in Qinghai—Tibet Plateau Meteorology*; Science Press: Beijing, China, 1988; ISBN 7030011066.
50. Sun, L.; Dong, X.; Zhou, Y.; Zhao, X.; Wang, G.; Chen, J. The Effect of Embankment Slope Orientation along the Qinghai-Tibet Routes and Routes and Related Radiation Mechanism. *J. Glaciol. Geocryol.* **2008**, *30*, 610–616. (In Chinese)
51. Sun, H. *The Formation and Evolution of the Qinghai—Tiebt Plateau*; Shanghai Scientific & Technical Publishers: Shanghai, China, 1996; ISBN 9787532340231.
52. Cui, T.; Wang, L.; Zhao, J.; Jiang, L.; Zhang, A.; Long, E. Analysis of greenhouse effect on greenhouse buildings. *Refrig. Air-Cond.* **2005**, *z1*, 280–282. (In Chinese) [CrossRef]
53. Liang, R. Research on the Optimization Strategy of Solar Thermal Performance of Existing Building Atriums in Universities in Cold Regions. Master's Thesis, Shandong Jianzhu University, Jinan, China, 2022. (In Chinese)
54. Mulyani, R.; Kholidasari, I. Wardi, The impact of building orientation on energy use: A case study in Bung Hatta University, Indonesia. *Int. J. Real Estate Stud.* **2017**, *11*, 43–48.
55. Morrissey, J.; Moore, T.; Horne, R.E. Affordable passive solar design in a temperate climate: An experiment in residential building orientation. *Renew. Energy* **2011**, *36*, 568–577. [CrossRef]
56. Motamedi, S. Energy analysis of different toplights for office buildings in austin. In Proceedings of the World Renewable Energy Forum Conference, Denver, CO, USA, 13–17 May 2012.
57. Ghobad, L.; Place, W.; Cho, S. *Design Optimization of Square Skylights in Office Buildings*; AIVC: Ghent, Belgium, 2013.
58. Vujošević, M.; Krstić-Furundžić, A. The influence of atrium on energy performance of hotel building. *Energy Build.* **2017**, *156*, 140–150. [CrossRef]
59. *GB/T 18883-2022*; Indoor Air Quailty Standard. National Health Commission of the People's Republic of China: Beijing, China, 2022.